A New Strategy for Mitigating Pipeline Uplift in Liquefied Soils

Flessati, Luca; Marveggio, Pietro; Di Prisco, Claudio; De Sarno, Domenico

DOI
10.1061/JPSEA2.PSENG-1459

Publication date
2023

Document Version
Final published version

Published in
Journal of Pipeline Systems Engineering and Practice

Citation (APA)
Flessati, L., Marveggio, P., Di Prisco, C., & De Sarno, D. (2023). A New Strategy for Mitigating Pipeline Uplift in Liquefied Soils. *Journal of Pipeline Systems Engineering and Practice*, *14*(4), Article 04023042. https://doi.org/10.1061/JPSEA2.PSENG-1459

ASCE

A New Strategy for Mitigating Pipeline Uplift in Liquefied Soils

Luca Flessati[1]; Pietro Marveggio[2]; Claudio di Prisco[3]; and Domenico De Sarno[4]

Abstract: Seismic-induced liquefaction is one of the main hazards for pipelines buried in saturated granular materials. When soil is partially or completely fluidized, a lifeline, although installed in superficial trenches in which the coarse backfill soil usually is compacted, may experience a sudden uplift and damages. To reduce pipeline uplift and thus limit the associated risks, the authors propose a sustainable and original mitigation strategy, suitable for both existing and new lifelines, based on both the use of a geomembrane and the compaction of the soil surrounding the pipeline. According to the design method proposed, the intervention geometry is selected on the basis of the pipeline maximum admissible displacement, whereas the minimum required relative density can be designed, based on the site-specific seismic demand, to avoid cyclically induced local accumulation in excess pore-water pressure. To prove the effectiveness of this strategy, a series of 1-g small-scale laboratory tests was performed on a pipe buried in a fluidized sand layer. A simplified displacement-based design approach, which was validated against the experimental data, is proposed. **DOI: 10.1061/JPSEA2.PSENG-1459.**

Author keywords: Buried pipelines uplift; Seismic-induced liquefaction; Sustainable risk mitigation; $1 = g$ small model tests; Displacement-based design; Geomembranes.

Introduction

In recent decades, the extent of buried pipelines for oil and gas distribution has increased exponentially. It is not rare that pipelines cross seismically active regions and pass through liquefiable strata. In this case, many authors have reported events of pipe uplift associated with soil partial or complete liquefaction (Yasuda et al. 1995; Koseki et al. 2000; Tobita et al. 2009; Chian and Tokimatsu 2012; Huang et al. 2014; Pisanò et al. 2020), causing structural damages, potentially impacting the infrastructure functionality, and, in the case of leakage of the transported fluid, impacting the surrounding environment as well.

The uplift phenomenon is caused by the partial or complete fluidization of the surrounding soil and the buoyancy of the pipe. Some authors have studied the problem experimentally (Yasuda et al. 1995; Koseki et al. 2000), but very few authors have studied it numerically (Della Vecchia et al. 2019; Pisanò et al. 2020). The numerical simulation requires the capability of dealing with large displacements and dynamic conditions, and the implementation of a constitutive relationship capable of describing the mechanical behavior of soils in both solid and fluidlike regimes (Vescovi et al. 2020; Marveggio et al. 2021; Marveggio et al. 2022).

In both the scientific literature and practical applications, different mitigation measures have been proposed to reduce the risks associated with pipe uplift. These can be subdivided into two categories: (1) mechanical, and (2) hydraulic interventions. In the former category are techniques aimed at (1) increasing the pipeline equivalent weight, (2) improving the mechanical properties of the surrounding soil, and (3) anchoring the pipeline. In the latter category are techniques aimed at locally reducing the pore-water pressure. This result usually is obtained by installing drains within the trenches in which the pipeline is buried.

The first category, which does not avoid the tendency of the soil close to the pipeline to liquefy, is aimed at balancing the buoyancy force exerted by the liquefied soil, coincident, according to Archimedes' principle, with the unit volume weight of the fluidized soil multiplied by the pipe volume. The most popular solution is based on the use of concrete to coat pipelines, obtaining a suitable equivalent unit volume weight, which is a function of the thickness of the coating layer. Alternatively, the pipeline weight may be increased by means of (1) cast in situ or precast concrete saddles, (2) saddlebags filled with sand or gravel, or (3) the installation of gravel bags above the pipeline (Ling et al. 2003; Castiglia et al. 2017, 2021). In all these cases, the materials employed to increase the weight are expected to be characterized by unit weight values not significantly larger than that of the saturated soil, implying that the volumes necessary to prevent uplift are very large. As a consequence, in many cases these mitigation techniques may be very expensive and not sustainable.

According to mitigation techniques based on soil improvement, standard injections (Andrus and Chung 1995), lime (Ito et al. 1994), or colloidal silica grout (Gallagher et al. 2007; Díaz-Rodríguez et al. 2008) have been proposed to create artificial intergranular bonds in the soil adjacent to the pipeline. These intergranular bonds, which provide shear strength even for zero effective stresses, prevent the local soil fluidization. When liquefaction takes place, the volume of the grouted soil along with the pipe behaves as a unique solid body.

[1]Assistant Professor, Faculty of Civil Engineering and Geoscience, Delft Univ. of Technology, Stevinweg 1, Delft 2628 CN, Netherlands. ORCID: https://orcid.org/0000-0002-9586-3057

[2]Assistant Professor, Dept. of Civil and Environmental Engineering, Politecnico di Milano, Piazza Leonardo da Vinci 32, Milano 20133, Italy (corresponding author). ORCID: https://orcid.org/0000-0002-9938-0220. Email: pietro.marveggio@polimi.it

[3]Full Professor, Dept. of Civil and Environmental Engineering, Politecnico di Milano, Piazza Leonardo da Vinci 32, Milano 20133, Italy.

[4]Onshore Geohazard Engineer, Saipem S.p.A, Via G. Toniolo, 1A, Zona Industriale Bellocchi, PU 61030, Italia.

Note. This manuscript was submitted on November 22, 2022; approved on July 10, 2023; published online on September 13, 2023. Discussion period open until February 13, 2024; separate discussions must be submitted for individual papers. This paper is part of the ***Journal of Pipeline Systems Engineering and Practice***, © ASCE, ISSN 1949-1190.

The grouted subdomain dimension necessary for preventing the uplift usually is very large and, again, even these mitigation measures are considered to be expensive and not sustainable.

In principle, the goal of anchoring techniques is to avoid pipeline movement by employing structural elements, such as screw anchors installed in the proximity of the pipeline (Castiglia et al. 2017) and anchored in the soil far from the pipeline. However, because the area potentially undergoing fluidization is expected to be quite extended and is difficult to individuate, these techniques are not cost-effective.

In terms of hydraulic mitigation measures, the installation of drains in the proximity of the pipeline (Miyajima et al. 1992; Orense et al. 2003; Castiglia et al. 2021) is particularly effective in locally reducing the accumulation of excess pore-water pressure. However, this type of intervention design is not straightforward, and the use of a large number of drains make this technique very expensive.

This paper proposes a new economic and sustainable pipeline uplift mitigation technique (section "Description of the Proposed Mitigation Technique"), based on

1. compacting the trench backfill soil, the superficial layer surrounding the trench, and the cushion layer under pipeline system up to a relative density designed on the basis of the specific seismic demand of the site and on the cyclic behavior of the soil layer [for example, as suggested by Seed et al. (1985)], to prevent local cyclic pore-water pressure accumulation; and
2. installing a geomembrane to hydraulically isolate the portion of soil adjacent to the pipeline and increase the mass involved by the movement.

To prove the effectiveness of this mitigation technique, the authors performed a series of 1-g small-scale model tests in which increased pore-water pressure was induced by means of an upward stationary seepage. This choice is justified theoretically in the section "Description of the Proposed Mitigation Technique," in which the natural phenomena associated with seismically induced soil liquefaction are discussed with reference to shallow buried pipelines in the case of sufficiently dense backfill materials. For the sake of completeness, the experimental setup is described briefly in the section "Description of the Experimental Setup." Experimental results initially were gathered without any mitigation system (section "Unmitigated Conditions: Experimental Tests and Interpretative Model"). Those data were adopted as reference for discussing the effectiveness of the proposed mitigation measure (section "Mechanical Displacement Mitigation Technique: Experimental Tests and Design Method"), for which a simplified interpreting approach, introduced by the authors and suitable for design purposes, is provided.

Description of the Proposed Mitigation Technique

The most dangerous consequence of seismic actions on saturated soil strata is a sudden increase in pore pressure, which in some cases causes material fluidization. This may be induced by either (1) cyclic accumulation of excess pore-water pressure (potentially inducing cyclic liquefaction), or (2) severe vertical seepage (potentially inducing soil piping).

Cyclic liquefaction takes place only during a seismic event (coseismic phenomenon), and depends on relative density and the number and amplitude of cycles [Fig. 1(a)] (Castro 1975; Seed and Booker 1977). The phenomenon may develop under practically undrained conditions, that is, when the rate of accumulation of excess pore-water pressure (a function of the relative density and the number and amplitude of cycles) is larger than rate of its dissipation (depending on soil permeability and soil stratum distance from the water table level (Seed and Booker 1977; Ishihara 1985). The pioneering works of the 70 s and 80 s focused on studying the local material behavior. More recently, using either centrifuges or shaking tables, the response of boundary value problems was investigated (Fiegel and Kutter 1994; Steedman and Sharp 2001; Adalier and Elgamal 2005; Brennan and Madabhushi 2005; Ueng and Chen 2006; Tohumcu Özener et al. 2009; Huang et al. 2014), and the results of these tests, considering both homogeneous and stratified layers (from loose to medium-dense conditions) confirmed the experimental findings at the representative elementary volume scale. Among these studies, (1) Fiegel and Kutter (1994) and Brennan and Madabhushi (2005) considered even the presence of a superficial silty layer, and (2) Huang et al. (2014) investigated the cyclic accumulation of excess pore-water pressure in the proximity of a pipeline buried in a homogeneous medium-dense layer. In this second case, the accumulation of excess pore-water pressure

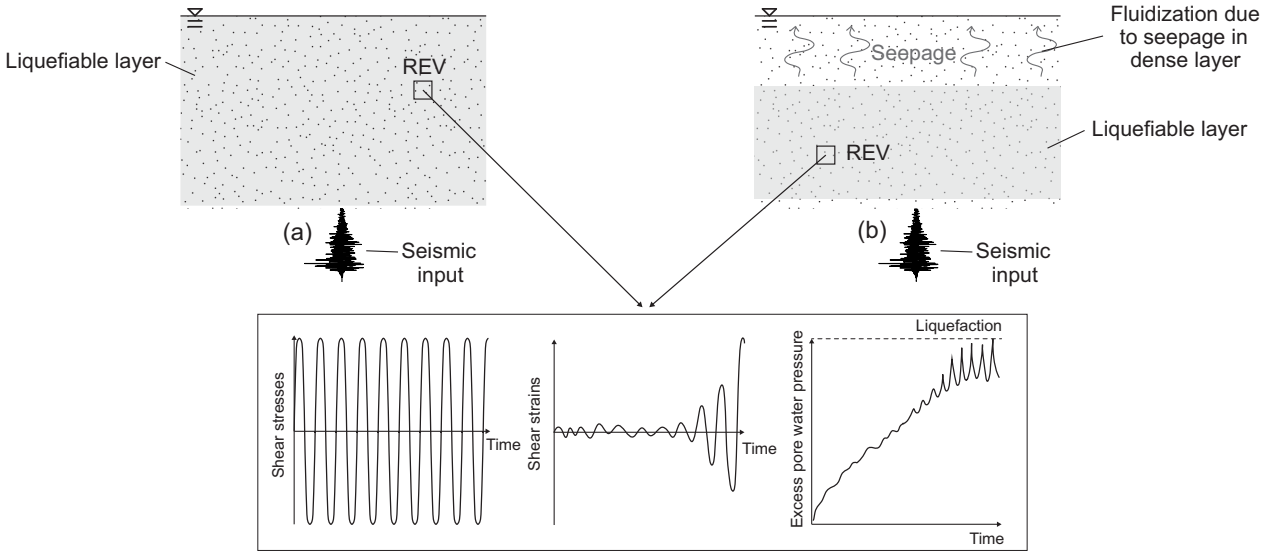

Fig. 1. (a) Liquefaction due to the accumulation of excess pore-water pressure; and (b) fluidization due to vertical upward seepage. REV = representative elementary volume.

J. Pipeline Syst. Eng. Pract., 2023, 14(4): 04023042

is affected locally by the presence of the pipe, with negligible effects on the global cyclic-induced fluidification mechanism. The experimental results clearly showed that pipeline uplift occurs with a sufficient reduction of effective stresses, but not necessarily with their nullification.

Piping [Fig. 1(b)] may take place both during and after a seismic event (postseismic phenomenon) in stratified soils, in which a loose granular material is covered by a very dense (not liquefiable) granular layer (Seed and Lee 1966; Ambraseys and Sarma 1969; Seed et al. 1975, 1985; Seed and Booker 1977).

Onshore pipelines usually are buried in shallow trenches (1–2 m deep) filled with compacted soils. The compaction can be designed to prevent, for any given design seismic event (in terms of amplitude and number of cycles), a severe increase in pore-water pressure in the proximity of the pipeline. In contrast, compaction cannot avoid pore-water pressure increase due to upward seepage and the activation of the consequent pipeline uplift. To reduce the vertical uplift of the pipe, a new technique based on the hydraulic isolation of the soil adjacent to the lifeline (Fig. 2, Subdomain A) from the rest of the surrounding domain (Fig. 2, Subdomain B) is introduced in this paper. This can be achieved by positioning a membrane impervious to water (geomembrane) in the trench employed to install the pipeline. To both limit construction costs and improve the intervention sustainability, the trench may be filled with the soil resulting from the excavation, suitably compacted to avoid its cyclic liquefaction.

The proposed mechanical displacement mitigation (MDM) technique has two different versions (MDMa and MDMb): the former (in which the membrane is positioned beneath the pipeline) is suitable for newly constructed pipelines [Fig. 2(a)], whereas the latter (in which the membrane is positioned partially above the pipeline), does not require the removal of soil beneath the pipeline, and thus is suitable even for existing pipelines [Fig. 2(b)].

The hydraulic isolation prevents the increase in pore-water pressure in the soil placed around the pipe, independent of the triggering mechanism.

In contrast with what was observed in the unmitigated case (section "Unmitigated Conditions: Experimental Tests and Interpretative Model"), when pore-water pressure in Subdomain B increases sufficiently, the uplift involves both the pipeline and Subdomain A. The combination of the two domains is characterized by an equivalent unit volume weight slightly smaller than that of the fluidized soil and significantly larger than the pipeline equivalent unit volume weight. Thus, the proposed mitigation measure cannot inhibit the inception of the uplift mechanism, but, as is shown in the section "Mechanical Displacement Mitigation Technique: Experimental Tests and Design Method," it severely reduces the final pipeline upward displacement u_f.

Description of the Experimental Setup

The main goal of this research was to prove the effectiveness of the proposed mitigation measure, not to describe the complex hydromechanical phenomena taking place locally when the uplift of the pipe takes place. Therefore, the authors induced the increase in pore-water pressure within the soil domain by imposing an upward seepage. For this, they performed a series of 1-g small-scale model tests. The experimental setup (Figs. 3 and 4) consisted of a box filled with a sandy layer, in which the pipe initially was buried. Optical sights were connected rigidly to the pipe by means of a vertical hollow brass rod, and a laser sensor device (LK-G402, Keyence Corporation of America, Itasca, Illinois) with a $\pm$100-mm measuring range and 2-μm repeatability was employed to measure vertical displacements directly.

The box was filled with a moist tamped 150-mm thick Ticino sand (Table 1) stratum (Fig. 3). A series of preliminary experimental tests, not reported here for the sake of brevity, allowed imposing, with satisfactory reproducibility, a uniform relative density corresponding to a saturated unit weight (γ_{sat}) of 18.2 kN/m^3. The authors used a standard compaction procedure, and for each test measured the material relative density along the depth by embedding in the soil small open-headed boxes of known volume. At the end of the test, their net weight was measured. These measures are omitted here for the sake of brevity.

The upward seepage process was induced by controlling the water pressure distribution at the base of the domain. To provide a uniform water flux, a 50-mm-thick gravel layer was positioned beneath the sand stratum [Fig. 3(a)]. Uniformity in water flux was verified by performing a series of preliminary seepage tests (without the pipe); 14 tests were performed, during which the hydraulic head was measured locally using 9 piezometers at different locations (on a 3×3 grid). At constant depth, all the measures coincided. During these tests, the outflow rate was measured, and, as was expected, before liquefaction the flow rate linearly depend on the hydraulic gradient imposed. To avoid infiltration of sand

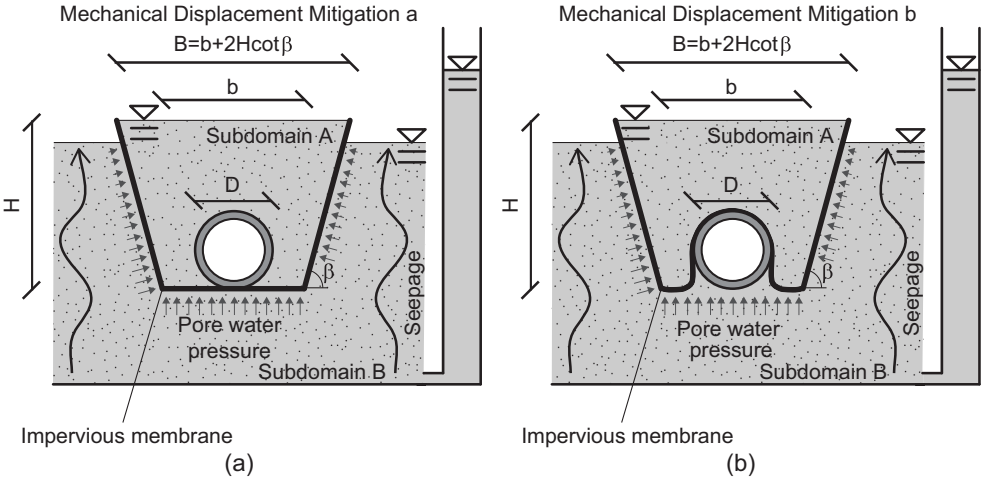

Fig. 2. Sketch of the mechanical mitigation: (a) membrane below the pipeline (MDMa); and (b) membrane above the pipeline (MDMb).

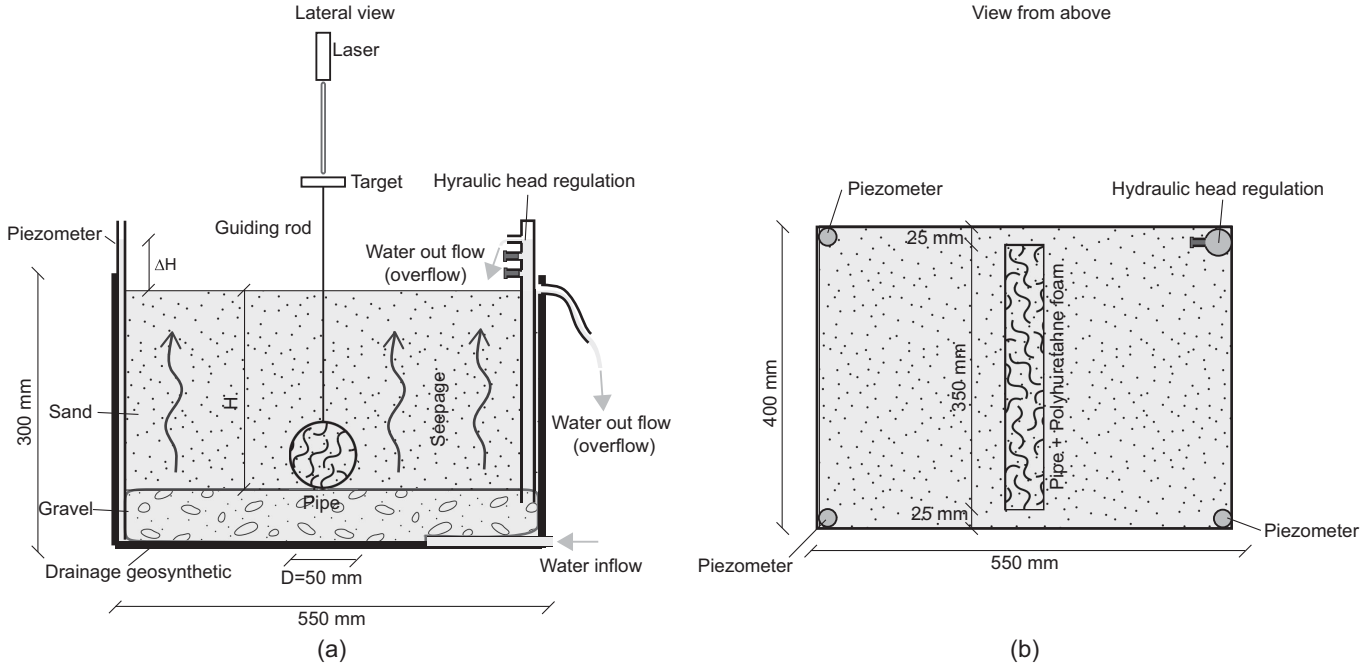

Fig. 3. Sketch of the experimental setup: (a) lateral view; and (b) view from above.

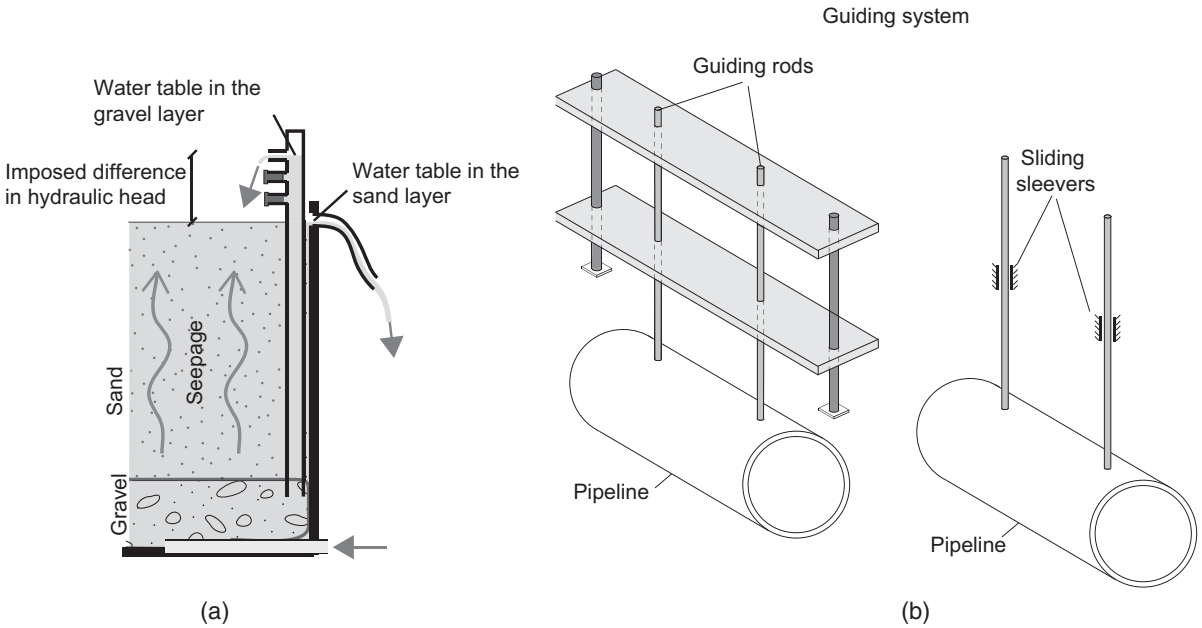

Fig. 4. Details of the experimental apparatus: (a) water regulation system; and (b) guiding system.

grains into intergranular gravel voids, a permeable geosynthetic layer (200 g/m^2, 1.6 mm thick, 100-μm characteristic opening, and 6-cm/s permeability) was positioned at the sand–gravel interface. To control and fix the water table level in both the sand and the gravel layers, two different overflow systems were installed [Fig. 4(a)]. To monitor the uniformity of pressure distribution at the base of the sand layer, three piezometers were positioned at three corners of the box [Fig. 3(b)].

The pipe was made of PVC (density 1.38 g/cm^3) and had an external diameter (D) of 50 mm and a thickness of 2 mm. To avoid soil and water intrusion in the pipe, it was filled with polyurethane foam. To avoid friction between pipe bases and box surfaces, the pipe length was 350 mm, slightly less than the box dimension (Fig. 3). The pipe equivalent unit weight (γ_{eq}) was 2.57 kN/m^3. As a precautionary measure, to avoid pipe rotation the pipe was connected rigidly to two hollow guiding rods made of brass (external diameter 3.5 mm, and 0.5 mm thick) and to a guiding system [Fig. 4(b)].

The results obtained were interpreted by assuming that the system behaved under plane strain conditions, because the value for the pipe length–diameter ratio, 7, was sufficiently large that boundary effects were negligible.

Table 1. Properties of Ticino sand (Fioravante 2000)

G_s	D_{50} (mm)	U_c	e_{min}	e_{max}	Morphology	Mineralogy
2.681	0.55	1.5	0.578	0.927	Angular (20%), subangular (55%), subrounded (25%)	Quartz (30%), feldspar (30%), mica (5%), opaque (35%)

Unmitigated Conditions: Experimental Tests and Interpretative Model

Test Procedure

In the unmitigated case, the test preparation (Fig. 5) consisted of

1. Trench excavation [Fig. 5(a)]—the moist tamped sand initially was partially saturated, so that a trench with vertical sides could be constructed.
2. Pipe positioning [Fig. 5(b)]—the pipe was positioned at the base of the trench. The distance between the base of the trench and the ground surface is hereafter named H.
3. Backfill deposition [Fig. 5(c)]—the soil was deposited over the pipe through moist tamping.
4. Soil saturation [Fig. 5(d)]—a low-gradient upward seepage was imposed for 24 h.

The test was performed by progressively increasing the hydraulic head at the base of the gravel layer. The test ended when the pipe stopped moving.

Different H/D ratio values (1.5, 2, 2.5, and 3) and different (only in terms of the final value of imposed gradient) hydraulic head versus time histories were considered.

Test Results

During the test, the controlled variable was the value of the average hydraulic gradient i (calculated as the ratio of imposed hydraulic head difference to the sand stratum thickness, $\Delta u_w/\gamma_w z$, where Δu_w is the local increase in pore-water pressure, z is the depth, and γ_w is the water unit volume weight), whereas the measured variable is the vertical displacement u. A stepwise time (t) evolution of i was imposed. For the sake of clarity, the results of only one test are discussed here in detail; all the other curves were very similar, and are omitted for the sake of brevity. These results, relative to $H/D = 3$ and the i history of Fig. 6(a), are reported in Figs. 6(b and c). During the early stages of the test ($i < 0.7$) a tensioned wire was positioned at the ground surface [Fig. 7(a), white line].

The experimental results showed that initially (Fig. 6, A–B) the displacements induced by the hydraulic head increment were negligible and rate-independent. For $i = \hat{i} = 0.6$ (Fig. 6, B) the pipe started moving (uplift inception), even if fluidization had not yet taken place. This is shown in Fig. 7(b), where, at the ground surface, the tensioned wire was partially covered by the soil, which is signature of a vertical upward displacement of the soil above the pipe. By further increasing i [$i = i^*$ (Fig. 6, C)], soil fluidization occurred locally [Fig. 7(c)], and an unstable response was obtained. Finally (Fig. 6, D), the pipe reached the ground surface [Fig. 7(d)]. Local fluidization (close to the pipe) was observed for values

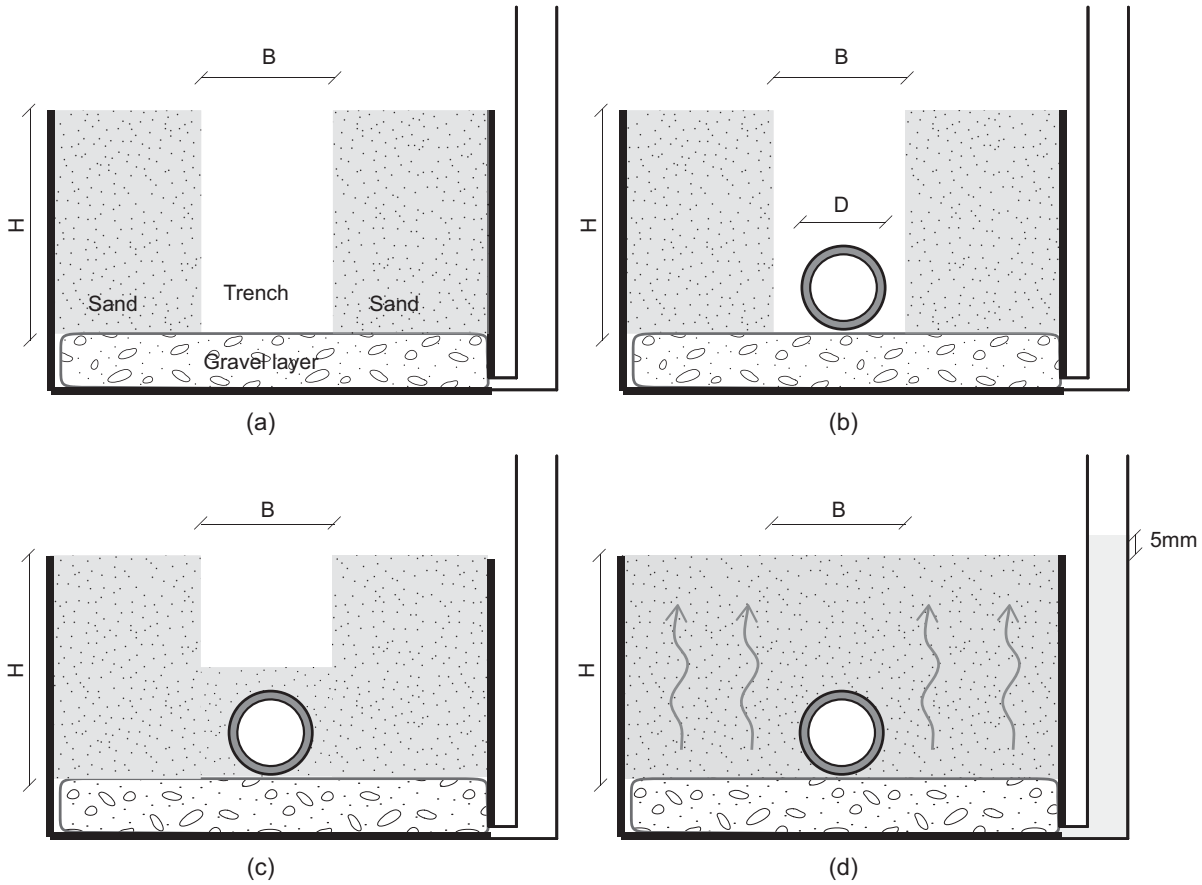

Fig. 5. Test preparation: (a) trench excavation; (b) pipe positioning; (c) backfill deposition; and (d) saturation.

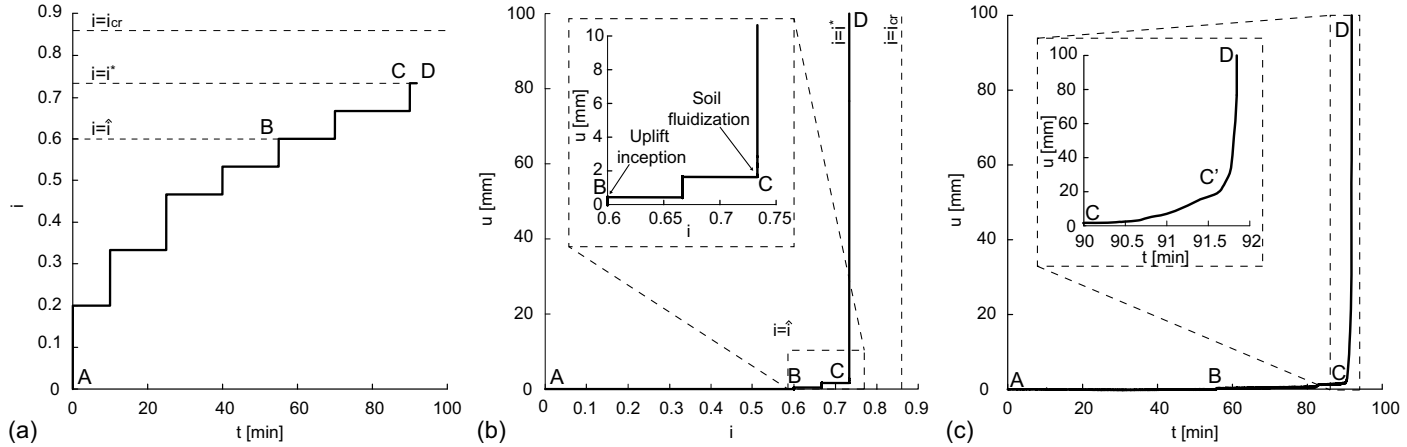

Fig. 6. (a) Imposed hydraulic gradient time history; (b) evolution of displacement with i; and (c) evolution of displacement with time ($H/D = 3$).

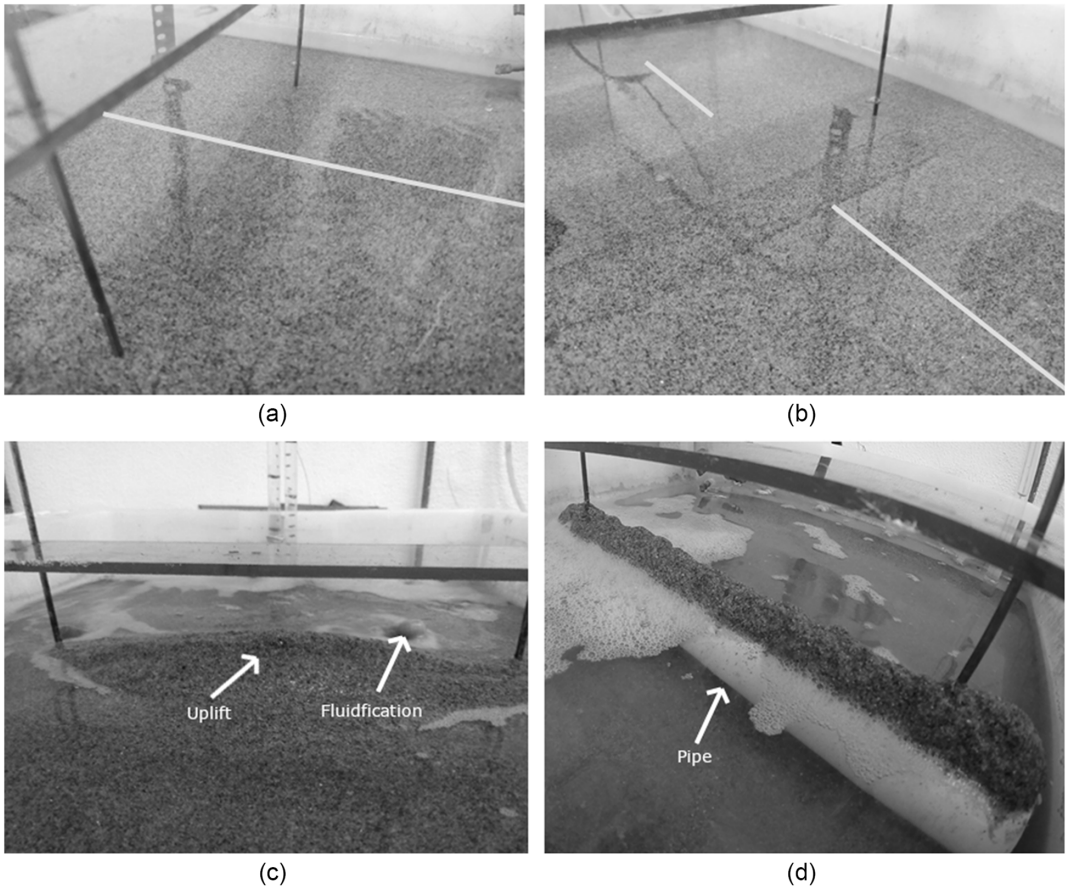

Fig. 7. Experimental results ($H/D = 3$): (a) initial condition (the white line indicates a tensioned wire); (b) uplift inception (Point B of Fig. 6); (c) fluidification (Point C of Fig. 6); and (d) complete pipe uplift (Point D of Fig. 6).

of i approximately equal to 85% of i_{cr}, which is the critical value of the hydraulic gradient associated with the nullification of vertical effective stresses in a one-dimensional case ($i_{cr} = \gamma'/\gamma_w$, where γ' is the soil submerged unit volume weight). To highlight the final response (CD), Fig. 6(c) includes an enlargement of the u-t curve as an inset. Initially, [Fig. 6(c), CC′] the pipe moves at a constant rate. At a certain displacement value (Point C′ for $u/D = 0.4$) the pipe velocity starts increasing (C′D). This unstable pipe uplift seems to be induced by the development of a cavity filled with water beneath the pipe (Schupp et al. 2006; Koseki et al. 2000; Cheuk et al. 2008). This cavity is expected to act as a drain, locally inducing (1) an increase in the water flux in the proximity of the pipe (Ling et al. 2003), (2) an increase in the local hydraulic gradient, and (3) a severe local reduction in effective stresses.

As previously mentioned, the authors performed tests characterized by the same target i time histories [Fig. 6(a)], but the final i value imposed was different due to the complete pipe uplift.

The estimation of $\hat{i}$ is particularly interesting for mitigation measure design: if $\hat{i}$ is larger than the maximum expected i value associated with the design seismic event, mitigation measures are not necessary.

Interpretative Model

To investigate the dependency of $\hat{i}$ on geometry, the authors also performed a series of experimental tests for different H/D ratio values. The experimental $\hat{i}$ values are summarized in Fig. 8(a) (solid circles) in the i/i_{cr}, H/D-plane. The use of i/i_{cr} is particularly convenient because $i/i_{cr} = \Delta u_w/(\gamma' z) = r_u$, which is a variable commonly employed to quantify the effect of seismic actions on saturated granular soil strata (Seed and Booker 1977; Ishihara 1985; Fiegel and Kutter 1994; Brennan and Madabhushi 2005; Huang et al. 2014).

To assess theoretically the $\hat{i}$ values, the soil was assumed to behave like a solid, the limit equilibrium method was adopted, and a chimney-like failure mechanism analogous to that proposed by Trautmann et al. (1985) was employed. In particular, the subdomain at failure involves the pipe and the portion of the soil domain directly above the pipe [Fig. 8(b)]. Under quasi-static conditions, the forces acting on this subdomain are

- the pipe weight W_p;
- the weight of the soil above the pipe W_s;
- the resultant force of the pore-water pressure U (not present in Trautmann et al. 1985) calculated by assuming a one-dimensional seepage (i.e. the pore-water pressure distribution is assumed not to be significantly influenced by the presence of the pipe) (Appendix); and
- the resultant force of tangential stresses acting on the two vertical sides of the soil domain above the pipe T. These tangential stresses are calculated as

$$\tau = \sigma'_h \tan \phi'_{ss} = k_{ss} \sigma'_v \tan \phi'_{ss} \tag{1}$$

where ϕ'_{ss} = friction angle under simple shear conditions (Pisanò et al. 2016; di Prisco et al. 2020; di Prisco and Flessati 2021; Boschi et al. 2023; Flessati et al. 2023; Mangraviti et al. 2023a, b), calculated by assuming a zero dilatancy angle and by using the value of a critical state friction angle of 35°, experimentally derived by Fioravante (2000); σ'_v = vertical effective stresses, calculated by assuming the seepage process to be one-dimensional

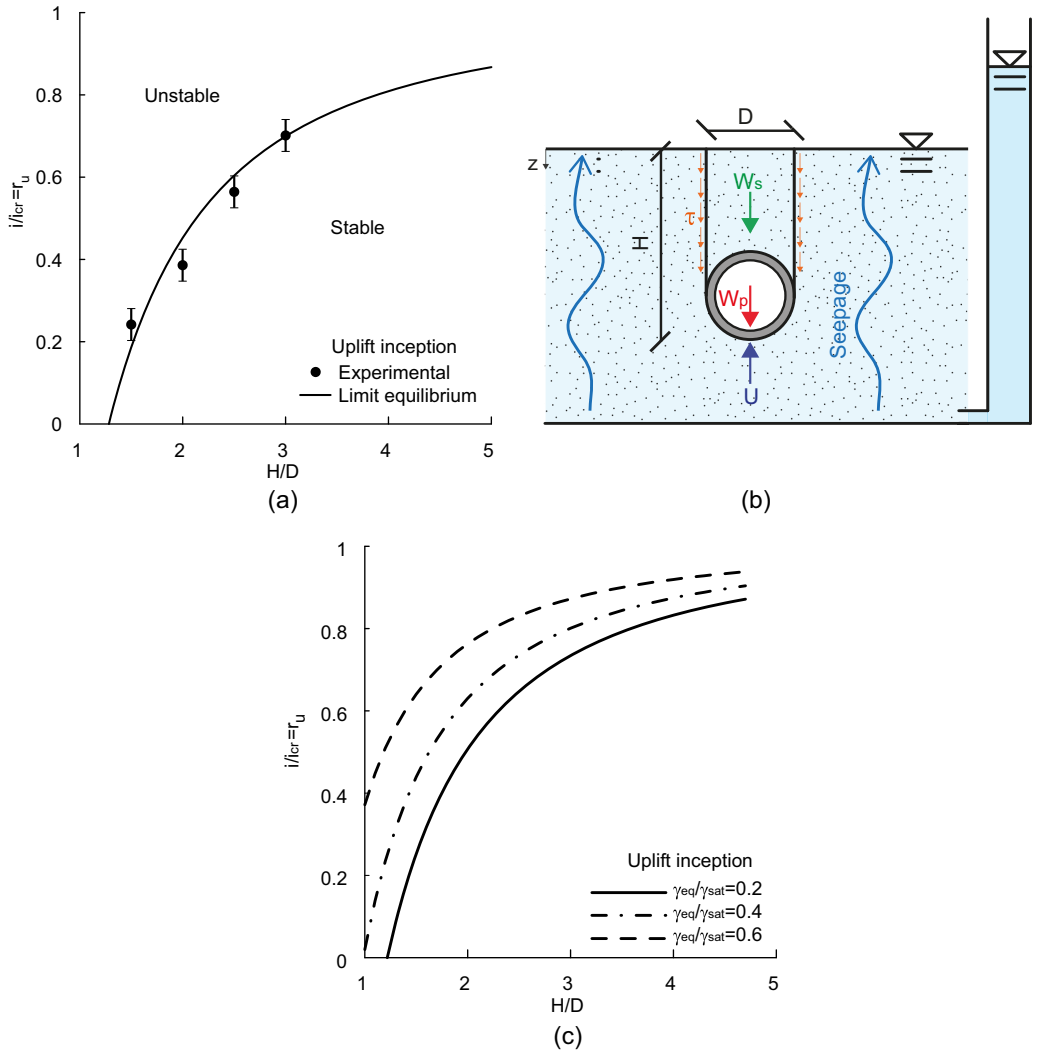

Fig. 8. (a) Variation of i on H/D comparison between experimental and limit equilibrium method results ($\gamma_{sat} = 18.2$ kN/m^3, $\gamma_{eq} = 2.57$ kN/m^3, $D = 5$ cm); (b) failure mechanism; (c) variation of i/i_{cr} with H/D for different γ_{eq}/γ_{sat} values ($\gamma_{sat} = 18.2$ kN/m^3, $D = 5$ cm).

J. Pipeline Syst. Eng. Pract., 2023, 14(4): 04023042

$$\sigma_v' = (\gamma' - i\gamma_w)z \tag{2}$$

By imposing the balance of momentum along the vertical direction

$$W_p + W_s + T = U \tag{3}$$

$\hat{i}$ is calculated as a function of k_{ss}. Due to the imposed vertical upward seepage, locally effective stresses are practically nil, and the solution is affected negligibly by k_{ss}. In this paper, k_{ss} was assumed to be equal to 1 (di Prisco and Pisanò 2011). The solid line of Fig. 8(a) corresponds to the solution of Eq. (3) for the geometry and soil properties of the case under consideration. The agreement with experimental results was very satisfactory. The theoretical assessment of $\hat{i}$ is expected to be conservative because it corresponds to the maximum value for which a static equilibrated configuration can be achieved.

For the sake of completeness, Fig. 8(c) shows the theoretical curves corresponding to different γ_{eq}/γ_{sat} values in typical ranges for practical applications. For practical purposes, Fig. 8(c) can be adopted as a design guide.

Mechanical Displacement Mitigation Technique: Experimental Tests and Design Method

Test Procedure

In case MDMa [Fig. 2(a)], which can be adopted for new lifelines only, the test preparation consisted of (1) trench excavation [Fig. 5(a)], (2) membrane positioning, (3) pipe positioning [Fig. 5(b)], (4) backfill deposition [Fig. 5(c)], and (5) saturation [Fig. 5(d)]. In case MDMb, which is suitable for both new and existing pipelines, Phases 2 and 3 were inverted.

As in the section "Unmitigated Conditions: Experimental Tests and Interpretative Model," the tests were performed by progressively increasing the hydraulic head at the base of the gravel layer. Even in this case, the imposed hydraulic gradient time history was characterized by a stepwise trend.

Test Results

The tests performed by the authors (Table 2) considered different geometries (different b/D and β values) and types of mitigation (MDMa or MDMb). In particular, two different values of b/D (1 and 3) and of β (45° and 90°) were taken into account.

The results of test MDM01 (MDMa), obtained by imposing the i versus time history reported in Fig. 6(a), were compared with the unreinforced case in Fig. 9(a). As was discussed in the section "Description of the Proposed Mitigation Technique," the proposed mitigation technique cannot completely inhibit the pipe uplift. Neither $\hat{i}$ nor i^* values are not significantly influenced by the presence of the membrane, because initially, from a mechanical point of view, the membrane does not play any role (its flexural stiffness is negligible under small displacements). However, the presence of the membrane significantly affects the system response after the onset of instability: in the unmitigated case the pipe continuously accelerates and reaches the ground surface [Fig. 7(d)]; in contrast, in the mitigated case, due to second-order effects, the pipe stops (for $u = u_f$) without reaching the ground surface. Figs. 9(b and c) plot the curves for MDM01–MDM04 to show the experimental test repeatability.

Fig. 9 also plots a curve corresponding to test MDM05, obtained using MDMb. This curve is similar to the curve corresponding to MDMa, suggesting that, from a practical point of view, the two versions of the mitigation measures seem to be equivalent.

The results of tests MDM06 and MDM07 ($b/B = 1$ and $\beta = 45°$) are compared with those of the nonmitigated case in Fig. 10(a). For the sake of completeness, Fig. 10(b) plots the results in the u, i-plane. Even in this case, (1) the proposed mitigation intervention could not completely inhibit the pipe uplift, (2) $\hat{i}$ and i^* were not significantly influenced by the presence of the membrane, and (3) the pipe stopped without reaching the ground surface.

In this case, the uplift of the inclined sides of the membrane [Fig. 10(b)], as observed by the authors, induced the formation of a preferential path for the water flow between the membrane and the soil underneath.

Table 2. Summary of experimental tests of mechanical mitigation

Tests	H/D	b/D	β (degrees)	Type of mitigation
MDM01–04	3	3	90	MDMa
MDM05	3	3	90	MDMb
MDM06–07	3	1	45	MDMa

Design Method

As was previously mentioned, the proposed mitigation technique does not influence $\hat{i}$, but rather the final displacement of the pipe. When instability occurred, in the unmitigated case the pipe moved within the (partially) fluidized soil and stopped only at the ground level when part of the pipe emerged. In other words, the final configuration was that corresponding to the satisfaction of static balance of momentum along the vertical direction (that is, buoyancy force became equal to the pipe weight). In contrast, in the mitigated case, after the onset of instability, the pipe moved along with Subdomain A of Fig. 2. Thus, the final configuration, corresponding again to the satisfaction of the static balance of momentum along the vertical direction, was obtained when the weight of pipe plus the soil in Subdomain A became balanced by the buoyancy force.

The proposed design approach is based on a modification of the standard limit equilibrium method, which accounts for large displacements. This relies on the following assumptions:

1. the membrane thickness and weight are negligible;
2. the system composed of the pipeline, membrane, and Subdomain A (Fig. 2) behaves as a unique rigid body;
3. Subdomains A and B remain hydraulically isolated even in the deformed configuration; and
4. the water pressure, depending on u_f, is equal to that obtained in the case of a one-dimensional vertical upward seepage process (Appendix), with $i = i_c$.

The use of i_c is justified by the aim of providing a safe side solution, because not only is i_c the maximum value for i, it also allows maximizing u_f.

The authors validated the model using the previously illustrated experimental test results corresponding to different b/D and β values. The authors wrote the governing equation in a nondimensional form and compared the results in the nondimensional u_f/D, B/D-plane (refer to Fig. 2 for definitions of B and D). The agreement was very satisfactory [Fig. 11(a)]. The use of these nondimensional variables is particularly convenient because the governing equation negligibly depends on β.

The same equation can be used for design purposes. Fig. 11(b) plots different curves corresponding to different γ_{eq}/γ_{sat} values. As is evident, u_f monotonically decreases with B (Fig. 2). Given D, H, and γ_{eq}/γ_{sat} as input data and an admissible system performance in

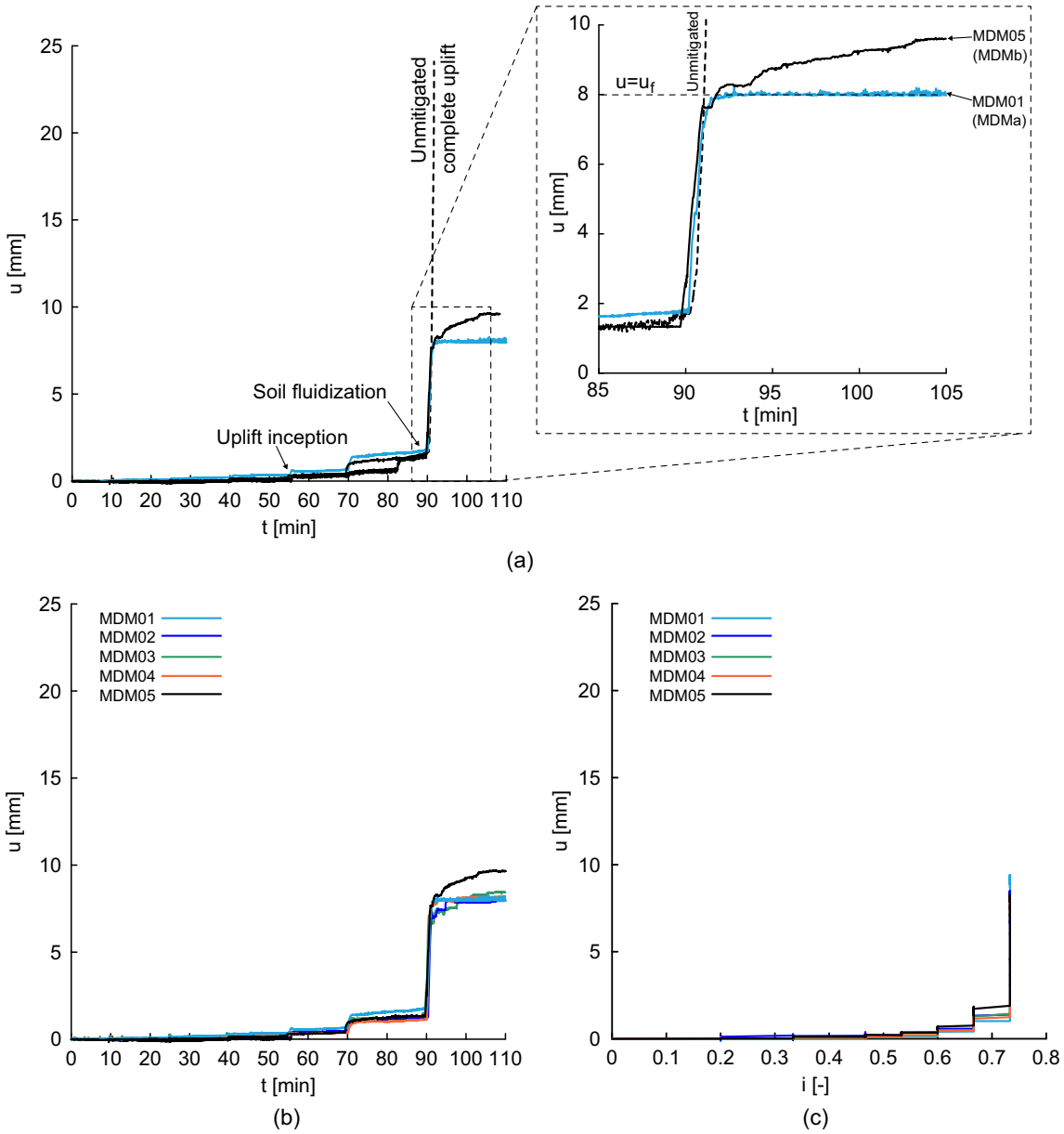

Fig. 9. Experimental results of tests MDM01–05.

terms of u_f, a unique B value is obtained. The value of β that minimizes the excavation volume (strictly related to the intervention cost) corresponds to $\beta = a\tan[2H - (B - \mathrm{D})]$, obtained by imposing $b = D$.

The mitigation technique, which was validated against small-scale experimental results, is expected to be reliable even in the case of real-scale pipelines, because it considers the final static equilibrated condition. In fact, because in the problem considered the effective stresses in the soil were practically nil, the well-known soil stiffness and strength stress dependence are expected to play a negligible role. In the case of larger pipelines, only the transient processes (reaching the ground surface in the unmitigated case, or reaching the final stable configuration in the mitigated case) are expected to be temporarily different. In particular, because the unstabilizing force is a volume force, whereas the (small) stabilizing forces (tangential stresses developing on either pipeline surface or membrane surface) are surface forces, transient processes are expected to be faster.

Concluding Remarks

This paper proposes a new strategy to mitigate the risk associated with the uplift of pipelines buried in fluidized or partially fluidized granular materials. The mitigation strategy consists of compacting the superficial soil layer in which the pipeline is installed to prevent local cyclic liquefaction and in laying down a membrane impervious to water in the trench in which the pipeline is installed. Compaction is essential to prevent liquefaction in the soil next to the pipeline, and must be designed according to the site-specific seismic demand and the cyclic soil behavior. The membrane counteracts the potential increase in pore-water pressure induced by seismic-induced upward seepage. The membrane may be placed either beneath or above the pipeline, for new or existing pipelines, respectively. The working principle of this mitigation measure consists of hydraulically isolating the soil placed in the coated trench. Therefore, the in situ soil may be employed as backfill material, drastically reducing the costs. A direct comparison of the

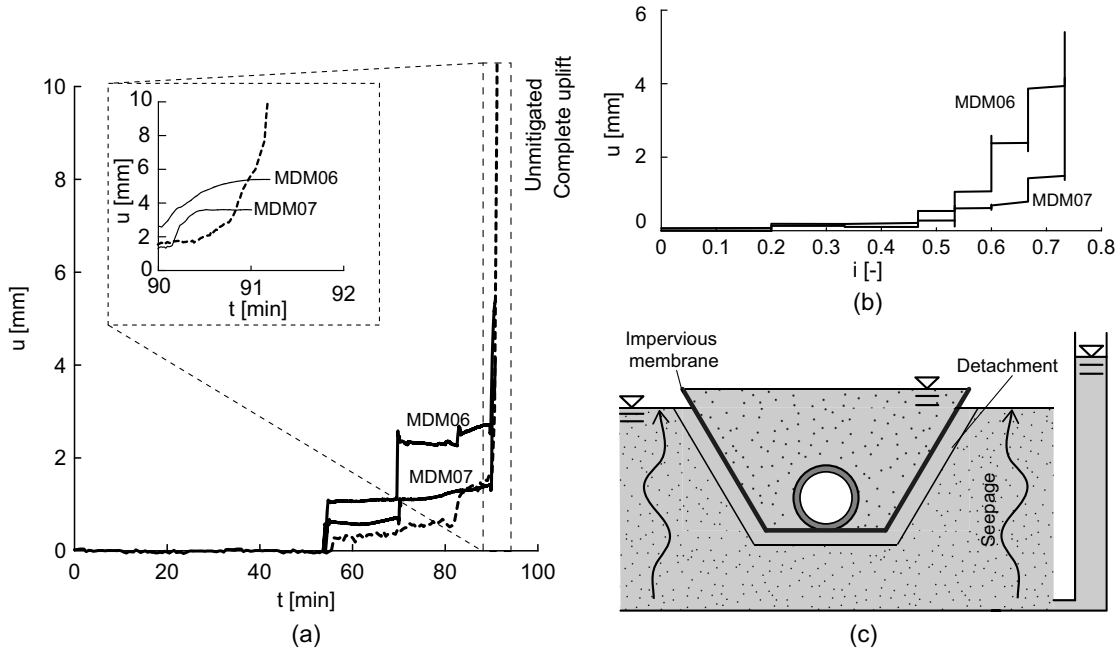

Fig. 10. Experimental results of tests MDM06 and MDM07: (a) displacement versus time; (b) displacement versus imposed hydraulic gradient; and (c) detachment of the membrane from the soil underneath.

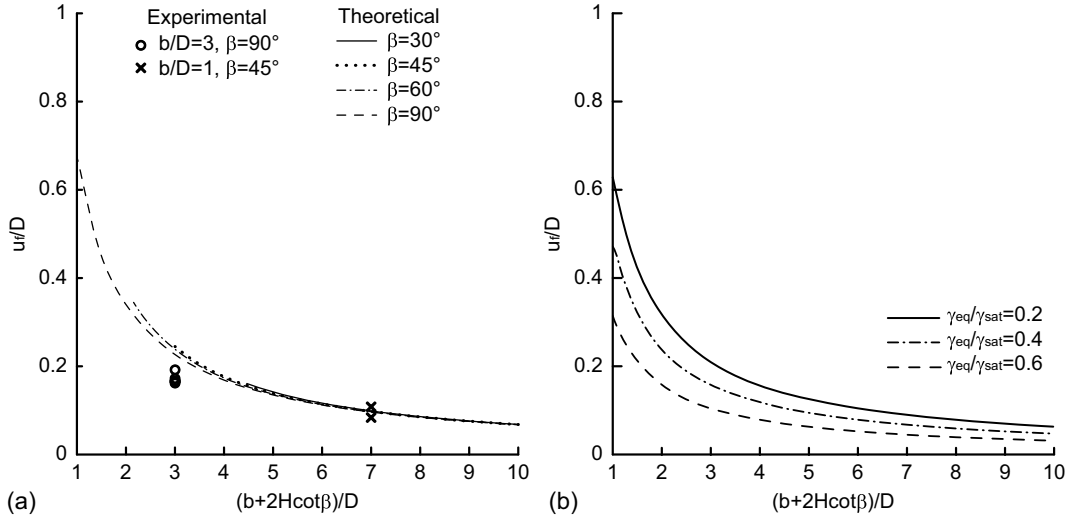

Fig. 11. (a) Theoretical and experimental results; and (b) influence of γ_{eq}/γ_{sat} on the final pipe displacement.

costs associated with this novel mitigation measure and the traditional measures is very site-specific, and was out of the scope of this paper.

Small-scale 1-*g* model tests, aimed at validating the mitigation measure effectiveness, consisting in imposing upward seepage to induce an increase in pore-water pressure in the soil surrounding the pipe, were carried out. The proposed technique was proven not to influence the uplift phenomenon inception, but to significantly reduce the final upward displacements. In the unmitigated case, the pipe always reached the ground level, whereas in the mitigated case, the final upward displacement is a function of the geometrical configuration employed for the membrane. This implies that membrane geometry can be designed to obtain a target system performance in terms of admissible upward pipeline displacements.

Regarding the inception condition, the limit equilibrium method, suitably modified to account the seepage process for, was employed to evaluate the gradient (increase in excess water pressure) for which uplift occurs. The theoretical predictions, validated against experimental test results, are particularly useful for determining whether mitigation is necessary or not.

In the mitigated case, to estimate final displacements, the static balance of momentum along the vertical direction was employed with reference to the deformed configuration (final geometry), by considering a pipe and soil placed in the trench above the pipe to behave as a unique rigid solid body. This approach, which was

validated against experimental test results, is a simple tool to be employed in the mitigation measure design. Given the geometry, pipe, and soil unit volume weights, this simple approach can be employed to design the geometry of the coated trench.

The mitigation measure is aimed at avoiding damages and interruption of services during and after extreme events. Potential aftershocks, which usually occur in a short period after the main event, are expected not to induce additional displacements to the mitigated system because during the main event a stable equilibrium condition is reached, and even if the surrounding soil is liquefied again, the pipeline is expected not to move.

Appendix. Seepage Analyses

The presence of the pipe necessarily modifies the pore-water pressure distribution within the soil. This appendix demonstrate that this modification is negligible, even if the trench is coated with the impervious membrane [Figs. 12(a–c)]. A series of two-dimensional (2D) linear numerical seepage analyses was performed using the commercial code Midas GTS NX version 2021 1.1. The spatial discretization, optimized by means of a series of preliminary analyses, which are not reported for the sake of brevity, was composed of 7,000 six-node triangular elements. The materials were assumed to obey Darcy's law and to be hydraulically isotropic. On the upper and lower boundaries of the domain, the hydraulic head was imposed to be constant; the difference in the imposed hydraulic head was $L = 4D$, where L is defined in Figs. 12(a–c). Both the pipe and the vertical boundaries of the domain were assumed to be impervious to water. The presence of the impermeable membrane [Figs. 12(b and c), RST] was simulated with an interface impervious to water.

The results of the simulations are reported in terms of flow nets [Figs. 12(a–c)] and contours of the normalized pore-water pressure ($u_w/\gamma_w L$) [Figs. 12(d–f)]. For the sake of clarity, Figs. 12(g–i) plot the profiles of u_w along depth (z) for Section P-P′ of Figs. 12(a–c) with reference to the three geometries taken into account.

In the nonmitigated case [Figs. 12(a, d, and g)], even if a slight curvature is observed in the equipotential line in the proximity of

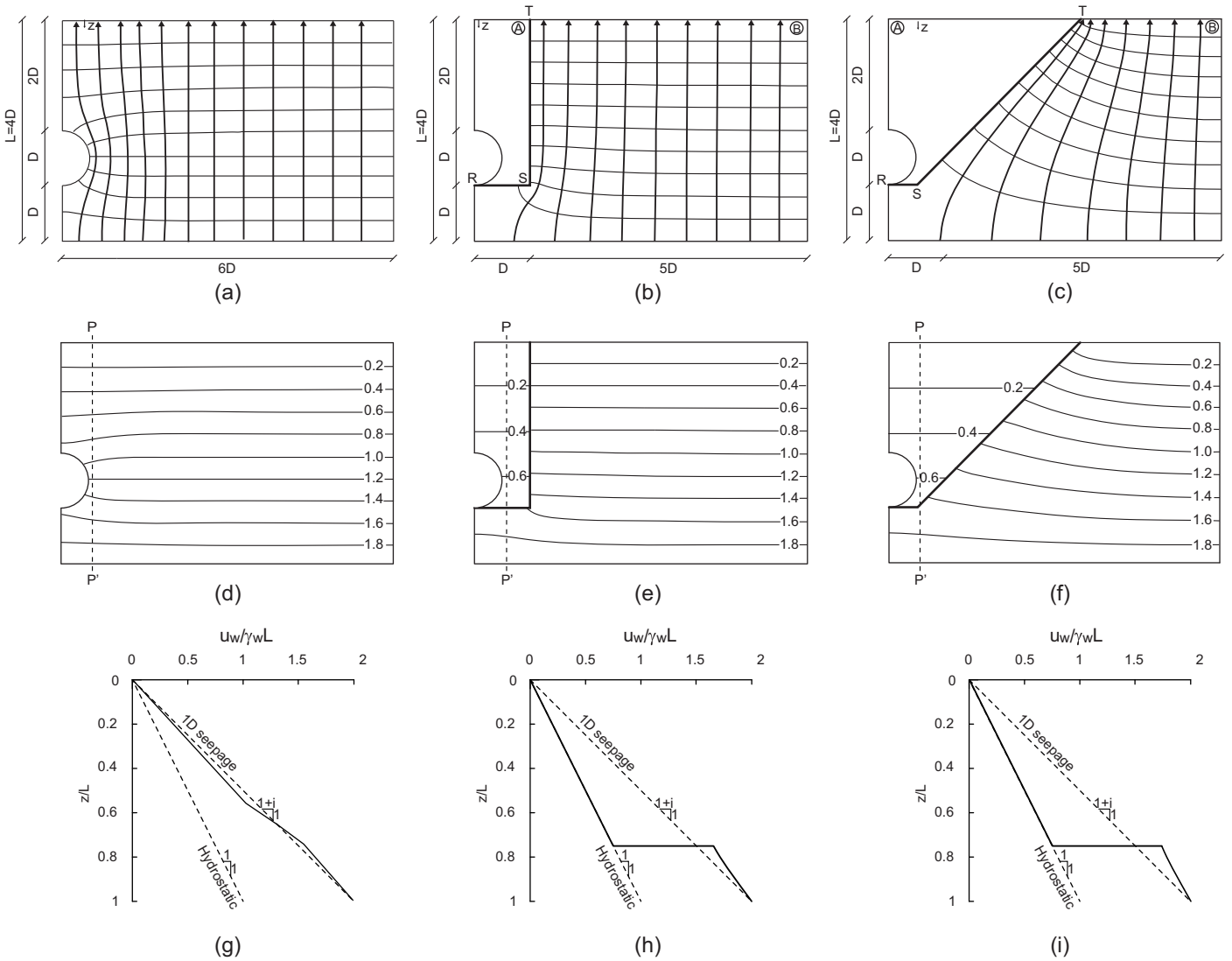

Fig. 12. Seepage numerical results: (a) flow net for unmitigated case; (b) flow net for MDMa and $\beta = 90°$; (c) flow net for MDMa and $\beta = 45°$; (d) normalized pore-water pressure for unmitigated case; (e) normalized pore-water pressure for MDMa and $\beta = 90°$; (f) normalized pore-water pressure for MDMa and $\beta = 45°$; (g) pore-water pressure distribution along PP′ for unmitigated case; (h) pore-water pressure distribution along PP′ for MDMa and $\beta = 90°$; and (i) pore-water pressure distribution along PP′ for MDMa and $\beta = 45°$.

the pipeline, the water pressure distribution was almost coincident with that obtained in a one-dimensional seepage process (the error is less than 5%).

The numerical results relative to the mitigated cases show that two subdomains can be distinguished, one within the impervious membrane [Figs. 12(b and c), Subdomain A] and one outside the membrane [Figs. 12(b and c), Subdomain B]. In Subdomain A, the hydraulic head is constant and the pore-water pressure is hydrostatic, implying that liquefaction is impossible, as was considered in the section "Description of the Proposed Mitigation Technique." In Subdomain B, the equipotential lines are almost horizontal and very slightly affected by the presence of the membrane. Considering the portion of domain adjacent to the membrane, the presence of the membrane tends to slightly increase the seepage force with respect to the far field, but this effect can be neglected because the relative difference in pore-water pressure $(|[u_w - (1+i)\gamma_w z]/[(1+i)\gamma_w z]|)$ for any z value is less than 10% [Figs. 12(h and i)].

Data Availability Statement

Some or all data, models, or code that support the findings of this study are available from the corresponding author upon reasonable request.

Acknowledgments

This research was funded by Saipem S.p.A. within the framework of an experimental and numerical program aimed at defining innovative design solutions for the mitigation of liquefaction-induced pipeline uplift. The authors thank Eng. F. Callea and Eng. M. Secondi for performing a part of the experimental campaign, and Dr. S. Alberti for his help in the conceptualization of the experimental apparatus.

References

Adalier, K., and A. Elgamal. 2005. "Liquefaction of over-consolidated sand: A centrifuge investigation." Supplement, *J. Earthquake Eng.* 9 (S1): 127–150. https://doi.org/10.1080/13632460509350582.

Ambraseys, N., and S. Sarma. 1969. "Liquefaction of soil induced by earthquakes." *Bull. Seismol. Soc. Am.* 59 (2): 651–664. https://doi.org/10.1785/BSSA0590020651.

Andrus, R. D., and R. M. Chung. 1995. "Liquefaction remediation near existing lifeline structures." In *Proc., 6th Japan-US Workshop on Earthquake Resistance Design of Lifeline Facilities and Countermeasures against Liquefaction*, 11–13. New York: US National Center for Earthquake Engineering Research.

Boschi, K., C. di Prisco, and F. Flessati. 2023. "Mechanical behaviour of anchored wire meshes: Numerical analyses and analytical modelling." *Acta Geotech*. https://doi.org/10.1007/s11440-023-02046-5.

Brennan, A., and G. Madabhushi. 2005. "Liquefaction and drainage in stratified soil." *J. Geotech. Geoenviron. Eng.* 131 (7): 876. https://doi.org/10.1061/(ASCE)1090-0241(2005)131:7(876).

Castiglia, M., F. S. de Magistris, F. Onori, and J. Koseki. 2021. "Mitigation systems for the uplift of buried pipelines in liquefiable soils under repeated shaking through model tests." *Soil Dyn. Earthquake Eng.* 148 (Sep): 106850. https://doi.org/10.1016/j.soildyn.2021.106850.

Castiglia, M., S. Morgante, A. Napolitano, and F. S. de Magistris. 2017. "Mitigation measures for the stability of pipelines in liquefiable soils." *J. Pipeline Eng.* 16 (3): 115–139.

Castro, G. 1975. "Liquefaction and cyclic mobility of saturated sands." *J. Geotech. Eng. Div.* 101 (6): 551–569. https://doi.org/10.1061/AJGEB6.0000173.

Cheuk, C. Y., D. J. White, and M. D. Bolton. 2008. "Uplift mechanisms of pipes buried in sand." *J. Geotech. Geoenviron. Eng.* 134 (2): 154–163. https://doi.org/10.1061/(ASCE)1090-0241(2008)134:2(154).

Chian, S. C., and K. Tokimatsu. 2012. "Floatation of underground structures during the Mw 9.0 Tōhoku earthquake of 11th March 2011." In *Proc., 15th World Conf. on Earthquake Engineering*. Red Hook, NY: Curran Associates.

Della Vecchia, G., M. Cremonesi, and F. Pisanò. 2019. "On the rheological characterisation of liquefied sands through the dam-breaking test." *Int. J. Numer. Anal. Methods Geomech.* 43 (7): 1410–1425. https://doi.org/10.1002/nag.2905.

Díaz-Rodríguez, J. A., V. M. Antonio-Izarraras, P. Bandini, and J. A. López-Molina. 2008. "Cyclic strength of a natural liquefiable sand stabilized with colloidal silica grout." *Can. Geotech. J.* 45 (10): 1345–1355. https://doi.org/10.1139/T08-072.

di Prisco, C., and L. Flessati. 2021. "Progressive failure in elastic–viscoplastic media: From theory to practice." *Géotechnique* 71 (2): 153–169. https://doi.org/10.1680/jgeot.19.P.045.

di Prisco, C., L. Flessati, G. Frigerio, and A. Galli. 2020. "Mathematical modelling of the mechanical response of earth embankments on piled foundations." *Géotechnique* 70 (9): 755–773. https://doi.org/10.1680/jgeot.18.P.127.

di Prisco, C., and F. Pisanò. 2011. "An exercise on slope stability and perfect elastoplasticity." *Géotechnique* 61 (11): 923–934. https://doi.org/10.1680/geot.9.P.040.

Fiegel, G. L., and B. L. Kutter. 1994. "Liquefaction mechanism for layered soils." *Int. J. Geotech. Eng.* 120 (4): 737–755. https://doi.org/10.1061/(ASCE)0733-9410(1994)120:4(737).

Fioravante, V. 2000. "Anisotropy of small strain stiffness of Ticino and Kenya sands from seismic wave propagation measured in triaxial testing." *Soils Found.* 40 (4): 129–142. https://doi.org/10.3208/sandf.40.4_129.

Flessati, L., C. di Prisco, M. Corigliano, and V. Mangraviti. 2023. "A simplified approach to estimate settlements of earth embankments on piled foundations: The role of pile shaft roughness." *Eur. J. Environ. Civ. Eng.* 27 (1): 194–214. https://doi.org/10.1080/19648189.2022.2035259.

Gallagher, P. M., A. Pamuk, and T. Abdoun. 2007. "Stabilization of liquefiable soils using colloidal silica grout." *J. Mater. Civ. Eng.* 19 (1): 33–40. https://doi.org/10.1061/(ASCE)0899-1561(2007)19:1(33).

Huang, B., J. Liu, P. Lin, and D. Ling. 2014. "Uplifting behavior of shallow buried pipe in liquefiable soil by dynamic centrifuge test." *Sci. World J.* 2014 (Jan): 1–16. https://doi.org/10.1155/2014/838546.

Ishihara, K. 1985. "Stability of natural deposits during earthquakes." In *Proc., 11th Int. Conf. on Soil Mechanics and Foundation Engineering*, 321–376. Milton Park, UK: Routledge.

Ito, T., Y. Mori, and A. Asada. 1994. "Evaluation of resistance to liquefaction caused by earthquakes in sandy soil stabilized with quick-lime consolidated briquette piles." *Soils Found.* 34 (1): 33–40. https://doi.org/10.3208/sandf1972.34.33.

Koseki, J., O. Matsuo, T. Sasaki, K. Saito, and M. Yamashita. 2000. "Damage to sewer pipes during the 1993 Kushiro-Oki and the 1994 Hokkaido-Toho-Oki earthquakes." *Soils Found.* 40 (1): 99–111. https://doi.org/10.3208/sandf.40.99.

Ling, H. I., Y. Mohri, T. Kawabata, H. Liu, C. Burke, and L. Sun. 2003. "Centrifugal modeling of seismic behavior of large-diameter pipe in liquefiable soil." *J. Geotech. Geoenviron. Eng.* 129 (12): 1092–1101. https://doi.org/10.1061/(ASCE)1090-0241(2003)129:12(1092).

Mangraviti, V., L. Flessati, and C. di Prisco. 2023a. "Geosynthetic-reinforced and pile-supported embankments: Theoretical discussion of finite difference numerical analyses results." *Eur. J. Environ. Civ. Eng.* https://doi.org/10.1080/19648189.2023.2190400.

Mangraviti, V., L. Flessati, and C. di Prisco. 2023b. "Mathematical modelling of the mechanical response of geosynthetic-reinforced and pile-supported embankments." *Int. J. Numer. Anal. Methods Geomech.* 47 (13): 2438–2466https://doi.org/10.1002/nag.3586.

Marveggio, P., I. Redaelli, and C. di Prisco. 2021. "A new constitutive approach for simulating solid- to fluid-like phase transition in dry and saturated granular media." In Vol. 116 of *Proc., 16th Int. Conf. of IACMAG*, 491–497. New York: Springer.

Marveggio, P., I. Redaelli, and C. di Prisco. 2022. "Phase transition in monodisperse granular materials: How to model it by using a strain hardening visco-elastic-plastic constitutive relationship." *Int. J. Numer. Anal. Methods Geomech.* 46 (13): 2415–2445. https://doi.org/10.1002/nag.3412.

Miyajima, M., M. Yoshida, and M. Kitaura. 1992. "Small scale tests on countermeasures against liquefaction for pipelines using gravel drain system." In *Proc., 4th Japan-US Workshop on Earthquake Resistant Design of Lifeline Facilities and Countermeasures for Soil Liquefaction*, 381–391. New York: US National Center for Earthquake Engineering Research.

Orense, R. P., I. Morimoto, Y. A. Yamamoto, T. Yumiyama, H. Yamamoto, and K. Sugawara. 2003. "Study on wall-type gravel drains as liquefaction countermeasure for underground structures." *Soil Dyn. Earthquake Eng.* 23 (1): 19–39. https://doi.org/10.1016/S0267-7261(02)00152-5.

Pisanò, F., M. Cremonesi, F. Cecinato, and G. Della Vecchia. 2020. "CFD-based framework for analysis of soil–pipeline interaction in reconsolidating liquefied sand." *J. Eng. Mech.* 146 (10): 04020119. https://doi.org/10.1061/(ASCE)EM.1943-7889.0001846.

Pisanò, F., L. Flessati, and C. Di Prisco. 2016. "A macroelement framework for shallow foundations including changes in configuration." *Géotechnique* 66 (11): 910–926. https://doi.org/10.1680/jgeot.16.P.014.

Schupp, J., B. W. Byrne, N. Eacott, C. M. Martin, J. Oliphant, A. Maconochie, and D. Cathie. 2006. "Pipeline unburial behaviour in loose sand." In Vol. 47497 of *Proc., Int. Conf. on Offshore Mechanics and Arctic Engineering*, 297–308. New York: ASME.

Seed, H. B., and J. R. Booker. 1977. "Stabilization of potentially liquefiable sand deposits using gravel drains." *J. Geotech. Eng. Div.* 103 (7): 757–768. https://doi.org/10.1061/AJGEB6.0000453.

Seed, H. B., and K. L. Lee. 1966. "Liquefaction of saturated sands during cyclic loading." *J. Soil Mech. Found. Div.* 92 (6): 105–134. https://doi.org/10.1061/JSFEAQ.0000913.

Seed, H. B., P. P. Martin, and J. Lysmer. 1975. *The generation and dissipation of pore water pressures during soil liquefaction*. Rep. No. EERC 75-26. Oakland, CA: Earthquake Engineering Research Center.

Seed, H. B., A. K. Tokimatsu, L. F. Harder, and R. M. Chung. 1985. "Influence of SPT procedures in soil liquefaction resistance evaluations." *J. Geotech. Eng.* 115 (12): 1425–1445. https://doi.org/10.1061/(ASCE)0733-9410(1985)111:12(1425).

Steedman, R. S., and M. Sharp. 2001. "Liquefaction of deep saturated sands under high effective confining stress." In *Proc., Int. Conf. on Recent Advances in Geotechnical Earthquake Engineering and Soil Dynamics*. Rolla, MO: Missouri Univ. of Science and Technology.

Tobita, T., S. Iai, G. C. Kang, and Y. Konishi. 2009. "Observed damage of wastewater pipelines and estimated manhole uplifts during the 2004 Niigata-Ken Chuetsu, Japan Earthquake." In *Proc., Technical Council on Lifeline Earthquake Engineering Conf. (TCLEE) 2009*. Reston, VA: ASCE.

Tohumcu Özener, P., K. Özaydın, and M. M. Berilgen. 2009. "Investigation of liquefaction and pore water pressure development in layered sands." *Bull. Earthquake Eng.* 7 (Mar): 199–219. https://doi.org/10.1007/s10518-008-9076-3.

Trautmann, C. H., T. D. O'Rourke, and F. H. Kulhawy. 1985. "Uplift force-displacement response of buried pipe." *J. Geotech. Eng.* 111 (9): 1061–1076. https://doi.org/10.1061/(ASCE)0733-9410(1985)111:9(1061).

Ueng, T. S., and C. H. Chen. 2006. "Liquefaction of sand under multidirectional shaking table tests." In *Proc., Int. Conf. on Physical Modelling in Geotechnics, ICPMG*, 481–486. Oxfordshire, UK: Taylor & Francis.

Vescovi, D., P. Marveggio, and C. G. Di Prisco. 2020. "Saturated granular flows: Constitutive modelling under steady simple shear conditions." *Géotechnique* 70 (7): 608–620. https://doi.org/10.1680/jgeot.19.P.023.

Yasuda, S., H. Nagase, S. Itafuji, H. Sawada, and K. Mine. 1995. "A study on the mechanism of the floatation of buried pipes due to liquefaction." *WIT Trans. Built Environ.* 14 (Jan): 15.